



Published in final edited form as:

N Engl J Med. 2009 May 7; 360(19): 1971–1980. doi:10.1056/NEJMoa0900082.

## STIM1 Mutation Associated with a Syndrome of Immunodeficiency and Autoimmunity

Capucine Picard, M.D., Ph.D., Christie-Ann McCarl, B.S., Alexander Papolos, B.S., Sara Khalil, B.S., Kevin Lüthy, Claire Hivroz, Ph.D., Françoise LeDeist, M.D., Ph.D., Frédéric Rieux-Laucat, Ph.D., Gideon Rechavi, M.D., Anjana Rao, Ph.D., Alain Fischer, M.D., Ph.D., and Stefan Feske, M.D.

From Assistance Publique–Hôpitaux de Paris, Hôpital Necker–Enfants Malades (C.P., F.L., A.F.), Laboratoire de Génétique Humaine des Maladies Infectieuses INSERM Unité 550, Necker Faculty (C.P.), Paris Descartes University (C.P., F.R.-L., A.F.), INSERM Unité 768 (C.H., F.L., F.R.-L., A.F.), and INSERM Unité 653 Curie Institut (C.H.) — all in Paris; New York, University School of Medicine, New York, (C.-A.M., A.P., S.K., K.L., S.F.); Centre Hospitalier Universitaire Sainte-Justine and University of Montreal, Montreal (F.L.); Chaim Sheba Medical Center and Sackler School of Medicine, Tel Aviv University, Tel Aviv, Israel (G.R.); and Immune Disease Institute and Harvard Medical School, Boston (A.R.).

### SUMMARY

A mutation in *ORAI1*, the gene encoding the pore-forming subunit of the  $\text{Ca}^{2+}$ -release-activated  $\text{Ca}^{2+}$  (CRAC) channel, abrogates the store-operated entry of  $\text{Ca}^{2+}$  into cells and impairs lymphocyte activation. Stromal interaction molecule 1 (STIM1) in the endoplasmic reticulum activates ORAI1–CRAC channels. We report on three siblings from one kindred with a clinical syndrome of immunodeficiency, hepatosplenomegaly, autoimmune hemolytic anemia, thrombocytopenia, muscular hypotonia, and defective enamel dentition. Two of these patients have a homozygous nonsense mutation in *STIM1* that abrogates expression of STIM1 and  $\text{Ca}^{2+}$  influx.

Combined Immunodeficiency Disease is a Rare Familial Disorder that can be caused by mutations in a variety of genes.<sup>1,2</sup> A principal feature of most cases of combined immunodeficiency disease is impaired function of T, B, or natural killer cells, despite their normal development. A defect in  $\text{Ca}^{2+}$ -dependent signaling in lymphocytes has been found in some types of immunodeficiency,<sup>1,2</sup> and here, we describe a newly discovered mutation that impairs lymphocyte activation in patients with combined immunodeficiency disease by disrupting  $\text{Ca}^{2+}$  entry into lymphocytes.

The release of  $\text{Ca}^{2+}$  from intracellular stores facilitates the influx of  $\text{Ca}^{2+}$  from the extracellular compartment, which is essential for activation of lymphocytes, by means of store-operated  $\text{Ca}^{2+}$ -entry channels. In T cells, these channels are CRAC channels.<sup>3–5</sup> The electrophysiological characteristics of CRAC channels include high  $\text{Ca}^{2+}$  selectivity and a gating mechanism that depends on the depletion of  $\text{Ca}^{2+}$  stores in the endoplasmic reticulum. Two molecules, STIM1 and ORAI1, mediate the function of CRAC channels and the store-operated entry of  $\text{Ca}^{2+}$  through them.<sup>6–10</sup> STIM1 senses the  $\text{Ca}^{2+}$  concentration in the endoplasmic reticulum and activates CRAC channels in the plasma membrane, and ORAI1 is

Copyright © 2009 Massachusetts Medical Society.

Address reprint requests to Dr. Feske at the Department of Pathology, New York University Langone Medical Center, 550 First Ave., New York, NY 10016, or at feskes01@nyumc.org.

Drs. Fischer and Feske contributed equally to this article.

the pore-forming subunit of the CRAC channel.<sup>11–13</sup> Our group reported previously that a missense mutation in *ORAI1*, resulting in a loss of CRAC-channel function and store-operated  $\text{Ca}^{2+}$  entry, causes a severe defect in T-cell activation and underlies combined immunodeficiency disease in two patients from one kindred.<sup>8,14</sup> Here, we describe three patients from one kindred with immunodeficiency, autoimmune hemolytic anemia, thrombocytopenia, muscular hypotonia, and disturbed enamel dentition. Two of these siblings, whose DNA was available for study, were homozygous for a recessive nonsense mutation in *STIM1* exon 3. The mutation results in a premature termination codon and consequent truncation of the STIM1 protein, which in turn leads to undetectable expression of the predicted STIM1 protein and defective store-operated entry of  $\text{Ca}^{2+}$ .

## CASE REPORTS

Patient V-1 was born at term to consanguineous parents from central Europe (Fig. 1A). Both parents and five sisters are healthy. Despite normal early cognitive development, the neonatal period of Patient V-1 was conspicuous because of partial iris hypoplasia and nonprogressive global muscular hypotonia (Table 1). Muscle biopsy and electromyography revealed no abnormalities. Lymphadenopathy and hepatosplenomegaly were apparent at 7 months of age; at 15 months she was found to have autoimmune hemolytic anemia, and at 5 years thrombocytopenia, both of which were treated with glucocorticoids. During the first 4 years of life, she had multiple infections caused by a spectrum of pathogens, including cytomegalovirus at 1 month of age, recurrent urinary tract infection, recurrent bacterial sepsis (caused by *Streptococcus pneumoniae* and *Escherichia coli*), and two episodes of chickenpox. After the age of 5 years, she had several episodes of otitis media and pneumonia. She also had a defect in enamel dentition, which became apparent in the first years of life. The patient died from complications of hematopoietic stem-cell transplantation, at 9 years of age.

Patient V-4 was the younger sister of Patient V-1. She had a clinical picture similar to that of her older sister, including severe autoimmune hemolytic anemia, thrombocytopenia, lymphadenopathy, hepatosplenomegaly, partial iris hypoplasia, and muscular hypotonia. She died from severe nephrotic syndrome that was resistant to therapy, encephalitis, and enterovirus infection, at the age of 18 months.

Patient V-7 is the brother of Patients V-1 and V-4. He had three undocumented episodes of sepsis during the first 2 months of life and was treated with intravenous immune globulin since birth. At 1 month of age, he had an episode of thrombocytopenia and at 2 years of age was found to have hypoglycemia. Patient V-7 survived after hematopoietic stem-cell transplantation (with a healthy, HLA-identical sister as donor) performed at 15 months of age, and intravenous immune globulin was stopped. He no longer has an increased susceptibility to infection. Currently, at 6 years of age, he has nonprogressive muscular hypotonia and partial iris hypoplasia only.

## METHODS

Written informed consent was obtained from the parents of the patients. The experiments were conducted after approval was given by the institutional review boards at New York University Langone Medical Center and Necker–Enfants Malades Hospital.

### Cell Lines And Plasmids

Fibroblasts from Patient V-1 and from controls were immortalized by means of retroviral transduction with human telomerase reverse transcriptase (hTERT), as previously described.<sup>8</sup> Cells were transduced with bicistronic retroviral expression vectors containing myc-epitope-tagged STIM1, STIM2, ORAI1, and internal ribosome entry site green fluorescent protein

(GFP), as previously described.<sup>8</sup> Protein expression was assessed by measuring the expression of GFP and immunoblotting for STIM1 with the use of peptide-specific antibodies.

### Genomic Sequencing

Genomic DNA from fibroblasts of Patient V-1 and from control fibroblast cell lines was isolated according to standard methods. For the polymerase-chain-reaction (PCR) assay, oligonucleotide primers flanking the exons of *STIM1* and *STIM2* encompassing splice sites were used; primer sequences are listed in Table 1 in the Supplementary Appendix (available with the full text of this article at NEJM.org). PCR products were amplified with the use of high-fidelity KOD DNA polymerase (EMD Biosciences), purified with the QIAquick gel extraction kit (Qiagen), and sent directly for sequencing (Genewiz). PCR and sequencing reactions were repeated three times from at least two independent genomic DNA preparations, if mutations were found. Sequence alignments were performed with the use of T-Coffee software (Swiss Institute of Bioinformatics); DNA-sequence traces were visualized with Xplorer software (version 1.0, dnaTools). Singlenucleotide polymorphism (SNP) searches were performed in the National Council for Biotechnology Information's dbSNP database (build 129; www.ncbi.nlm.nih.gov/SNP). Genomic DNA obtained from 50 white, healthy controls (representing a total of 100 chromosomes) were also sequenced.

Real-time PCR was done as previously described.<sup>14</sup> Primers used for the amplification of complementary DNA are listed in the Supplementary Appendix.

### Immunoblotting And Antibodies

Flow-cytometric analysis of lymphocytes, assays for the proliferation of peripheral-blood mononuclear cells, and the apoptosis assay were performed as previously described.<sup>17</sup> Serum immunoglobulin levels were determined by nephelometry. Immunoblotting was performed on the basis of standard protocols.<sup>14</sup> Antibodies against actin (sc-1616, Santa Cruz Biotechnology) and STIM1 (GOK, BD Biosciences) were purchased. A polyclonal antibody against the C-terminal domain of STIM1 was generated by immunizing rabbits with a conserved 29–amino acid peptide corresponding to amino acids 657 to 685 of human STIM1 (NP\_003147), according to standard protocols (Open Biosystems). Antisera were affinity-purified with the immunizing peptide. Single-cell measurements of intracellular Ca<sup>2+</sup> concentrations were obtained, as previously described.<sup>8</sup> Further details on experimental procedures are available in the Methods section of the Supplementary Appendix.

## RESULTS

### Immunologic Assessments

Lymphocyte counts for Patients V-1, V-4, and V-7 were slightly reduced or normal, with an age-appropriate distribution of lymphocyte subpopulations. Decreased proportions of naive CD4<sup>+</sup> T cells and CD4<sup>+</sup>CD45RA<sup>+</sup>CD31<sup>+</sup> T cells (recent emigrants from the thymus) were found for Patient V-1. Her T-cell repertoire was normal, as evaluated with the use of monoclonal antibodies against T-cell–receptor  $\beta$ -chain–variable regions (V $\beta$ 3, V $\beta$ 8, V $\beta$ 13-6, V $\beta$ 13-17, and V $\beta$ 21-3). The numbers of CD4<sup>+</sup>FOXP3<sup>+</sup> regulatory T cells were greatly reduced in blood specimens from Patient V-1 (Table 1, and Fig. 1 in the Supplementary Appendix). T-cell proliferation in response to phytohemagglutinin, phorbol 12-myristate 13-acetate plus ionomycin, or an anti-CD3 antibody was moderately to markedly reduced in Patients V-1 and V-7, and these two patients had severely impaired T-cell responses to recall antigens (varicella–zoster virus and tetanus toxoid), despite two episodes of chickenpox (in Patient V-1) and one round of vaccination against diphtheria, pertussis, and tetanus 1 month before testing of the response to recall antigens (in Patient V-7). T-cell apoptosis induced by Fas was normal in Patient V-1. Serum levels of IgG, IgA, and IgM were within or close to the

normal range in Patients V-1 and V-7, whereas IgG levels were greatly reduced in Patient V-4, most likely secondary to the nephrotic syndrome.

### Nonsense Mutation In *Stim1*

The stimulation of fibroblasts by thapsigargin, an inhibitor of the sarcoplasmic–endoplasmic reticulum  $\text{Ca}^{2+}$  ATPase, revealed a pronounced defect in store-operated  $\text{Ca}^{2+}$  entry in Patient V-1 as compared with controls (Fig. 1B). Normally, depletion of intracellular  $\text{Ca}^{2+}$  stores by thapsigargin activates store-operated  $\text{Ca}^{2+}$  entry through CRAC channels. The defect in this mechanism in fibroblasts of Patient V-1 resembles the defective store-operated  $\text{Ca}^{2+}$  entry in ORAI1 deficiency, in which CRAC channels are not functional.<sup>8,14</sup> However, genomic DNA sequencing failed to reveal mutations in *ORAI1* or its paralogues *ORAI2* and *ORAI3* in Patient V-1.

Biochemical analysis has shown that STIM proteins are required for the activation of ORAI channels,<sup>18,19</sup> and both RNA-interference experiments and transgenic mouse models show that STIM1 is essential for store-operated  $\text{Ca}^{2+}$  entry in many types of cells.<sup>6,7,20–23</sup> The sequencing of genomic DNA obtained from Patient V-1 for *STIM1* mutations revealed a 380\_381insA mutation, resulting in the insertion of an adenine in exon 3 of *STIM1* between positions 380 and 381 in the coding sequence (Fig. 1C). This mutation causes a frame shift that alters eight amino acids (RSIQLDRG) and results in a premature termination codon in *STIM1*. The same mutation was found in Patient V-7. The 380\_381insA mutation is not a known SNP (according to dbSNP, build 129) and was not found in 50 unrelated controls (data not shown). The predicted mutant protein, designated STIM1-E136X, is expected to be truncated at the beginning of a sterile alpha-motif (SAM) domain in the endoplasmic reticulum–luminal portion of STIM1 (Fig. 1D).

### Loss Of Stim1

Because premature termination codons often result in nonsense-mediated decay of messenger RNA (mRNA),<sup>24</sup> we analyzed mRNA transcript and protein levels for STIM1 in Patient V-1. We found significantly reduced *STIM1* mRNA levels in fibroblasts from Patient V-1 as compared with control fibroblasts ( $P = 0.04$ ), as measured by realtime reverse-transcriptase PCR (Fig. 2A). Transcript levels for *STIM2*, by contrast, were similar in fibroblasts from Patient V-1 and one control cell line. Expression of the full-length STIM1 protein was not detectable in fibroblasts from Patient V-1, as compared with cells from a control and a previously described patient with ORAI1 deficiency<sup>8</sup> (Fig. 2B). An antibody against the N-terminal end of STIM1 also failed to detect full-length STIM1 or the predicted mutant STIM1 fragment (approximately 15 kD in size) in cells from Patient V-1 (Fig. 3 in the Supplementary Appendix). Taken together, these data indicate that our patient's cells lack or have considerably reduced *STIM1* mRNA and protein.

To confirm the causative role of the nonsense *STIM1* mutation in defective store-operated  $\text{Ca}^{2+}$  entry, we transduced fibroblasts from Patient V-1 with wild-type *STIM1*, *STIM2*, *ORAI1*, or an empty vector using retroviral expression vectors that allow for bicistronic expression of GFP from an internal ribosome entry site. For analysis of  $\text{Ca}^{2+}$  influx, GFP-labeled cells were selected. Transduction with *ORAI1* failed to rescue the defect in the patient's fibroblasts, but expression of STIM1 rescued store-operated  $\text{Ca}^{2+}$  influx. A similar, although less robust, rescue of store-operated  $\text{Ca}^{2+}$  entry was seen after we transduced the patient's fibroblasts with wild-type STIM2 (Fig. 2C and 2D). A similar effect of STIM2 has been found in *Stim1*-deficient fibroblasts harvested from mouse embryos.<sup>21</sup> Nevertheless, the amount of endogenous STIM2 in the cells from Patient V-1 does not seem sufficient to compensate for the lack of STIM1.

## DISCUSSION

One of the strongest indications that  $\text{Ca}^{2+}$  influx through CRAC channels is essential for lymphocyte activation and immune responses comes from the study of rare inherited immunodeficiency syndromes involving defects in store-operated  $\text{Ca}^{2+}$  entry.<sup>8,14,25–27</sup> We describe three siblings with a complex immunodeficiency disorder, and detailed studies of one of them revealed reduced or absent STIM1 resulting from a nonsense mutation in *STIM1*. Whether Patient V-4 has the same mutation in *STIM1* is yet unknown but is plausible, because the clinical pictures for all three children were virtually the same.

STIM1 is required to activate store-operated  $\text{Ca}^{2+}$  entry in a variety of cells, including lymphocytes.<sup>6,7,20–23</sup> We found that fibroblasts from a patient with STIM1 deficiency have a severe defect in  $\text{Ca}^{2+}$  entry that was rescued by reintroducing wild-type STIM1 into the patient's cells. The clinical phenotype of the three patients with STIM1 deficiency is similar to that observed in two patients with a missense mutation in *ORAI1* (R91W), the pore-forming subunit of the CRAC channel. This mutation abrogates CRAC-channel activity and store-operated  $\text{Ca}^{2+}$  entry.<sup>8</sup> Patients with deficiencies in both STIM1 and ORAI1 have a primary immunodeficiency marked by susceptibility to viral and bacterial infections and also nonprogressive myopathy and defects in the formation of dental enamel. This overlap of clinical findings suggests that the phenotype resulting from mutations in *STIM1* and *ORAI1* is not genespecific but, rather, pathway-specific — that is, it reflects the lack of function of CRAC channels.

Of the three siblings we studied, two had autoimmune hemolytic anemia and immune thrombocytopenia; the third, a boy, had only one episode of thrombocytopenia. Other clinical features were hepatosplenomegaly, lymphadenopathy, and, in the boy, hypoglycemia. In mice in which both *Stim1* and *Stim2* had been deleted in T cells,<sup>21</sup> the phenotype consisted of splenomegaly, lymphadenopathy, organ infiltration by leukocytes, dermatitis, and blepharitis. This phenotype is attributed to a defect in the development and function of regulatory T cells caused by the defect in store-operated  $\text{Ca}^{2+}$  entry and depressed function of the nuclear factor of activated T cells (NFAT) protein.<sup>21</sup> It has been proposed that formation of a complex between the FOXP3 and NFAT transcription factors is required for the development of regulatory T cells.<sup>28</sup> Very low numbers of CD4+FOXP3+ T cells were detected in the blood specimens obtained from Patient V-1 (the only patient for whom blood specimens were available), and it is therefore possible that store-operated  $\text{Ca}^{2+}$  entry is required for differentiation of regulatory T cells in humans. The three siblings we describe did not have clinical features of the immune dysregulation, polyendocrinopathy, enteropathy, X-linked syndrome,<sup>29</sup> which is due to FOXP3 deficiency.

The nonprogressive muscular hypotonia seen in all three siblings correlates with a similar phenotype in patients with ORAI1 deficiency<sup>8</sup> and with the defect in muscle development and function in *Stim1*-deficient mice.<sup>20</sup> Muscle dysfunction is severe in such mice, and is probably responsible, at least in part, for the early death seen in *Stim1*- and *Orai1*-deficient mice.<sup>20–23,30</sup>

In summary, the clinical phenotype of the three siblings we studied, two of whom had a STIM1 deficiency due to a homozygous nonsense mutation in the *STIM1* gene, is remarkably similar to the phenotype of patients with ORAI1 deficiency. The lack of store-operated  $\text{Ca}^{2+}$  entry due to defects in ORAI1 or STIM1 interferes with immune function, causing immunodeficiency, autoimmune disease, and myopathy.

## Supplementary Material

Refer to Web version on PubMed Central for supplementary material.



## Acknowledgments

Supported by grants from the National Institutes of Health (NIH) (to Dr. Rao), from the March of Dimes Foundation and NIH (to Dr. Feske), and INSERM (to Drs. Rieux-Laucat and Fischer).

Drs. Rao and Feske report being scientific cofounders of Calci-Medica, a biotechnology company that seeks to develop CRAC channel inhibitors. No other potential conflict of interest relevant to this article was reported.

We thank Dr. Patrick G. Hogan for critical reading of a previous version of the manuscript; Corinne Jacques, Chantal Harre, Stephanie Ndaga, and Françoise Selz for their technical help; and Marie-Claude Stolzenberg for the immunophenotyping of regulatory T cells. We also thank Dr. Rochelle Hirschhorn (New York University Langone Medical Center) for providing DNA samples obtained from healthy controls and Silvia Menendez and Dr. Eva Hernando (both at New York University Langone Medical Center) for providing the control fibroblast cell lines.

## REFERENCES

1. Fischer A. Human primary immunodeficiency diseases. *Immunity* 2007;27:835–845. [PubMed: 18093537]
2. Geha RS, Notarangelo LD, Casanova JL, et al. Primary immunodeficiency diseases: an update from the International Union of Immunological Societies Primary Immunodeficiency Diseases Classification Committee. *J Allergy Clin Immunol* 2007;120:776–794. [PubMed: 17952897]
3. Feske S. Calcium signalling in lymphocyte activation and disease. *Nat Rev Immunol* 2007;7:690–702. [PubMed: 17703229]
4. Lewis RS. The molecular choreography of a store-operated calcium channel. *Nature* 2007;446:284–287. [PubMed: 17361175]
5. Oh-hora M, Rao A. Calcium signaling in lymphocytes. *Curr Opin Immunol* 2008;20:250–258. [PubMed: 18515054]
6. Liou J, Kim ML, Heo WD, et al. STIM is a  $Ca^{2+}$  sensor essential for  $Ca^{2+}$ -store-depletion-triggered  $Ca^{2+}$  influx. *Curr Biol* 2005;15:1235–1241. [PubMed: 16005298]
7. Roos J, DiGregorio PJ, Yeromin AV, et al. STIM1, an essential and conserved component of store-operated  $Ca^{2+}$  channel function. *J Cell Biol* 2005;169:435–445. [PubMed: 15866891]
8. Feske S, Gwack Y, Prakriya M, et al. A mutation in Orai1 causes immune deficiency by abrogating CRAC channel function. *Nature* 2006;441:179–185. [PubMed: 16582901]
9. Vig M, Peinelt C, Beck A, et al. CRACM1 is a plasma membrane protein essential for store-operated  $Ca^{2+}$  entry. *Science* 2006;312:1220–1223. [PubMed: 16645049]
10. Zhang SL, Yeromin AV, Zhang XH, et al. Genome-wide RNAi screen of  $Ca^{2+}$  influx identifies genes that regulate  $Ca^{2+}$  release-activated  $Ca^{2+}$  channel activity. *Proc Natl Acad Sci U S A* 2006;103:9357–9362. [PubMed: 16751269]
11. Prakriya M, Feske S, Gwack Y, Srikanth S, Rao A, Hogan PG. Orai1 is an essential pore subunit of the CRAC channel. *Nature* 2006;443:230–233. [PubMed: 16921383]
12. Vig M, Beck A, Billingsley JM, et al. CRACM1 multimers form the ion-selective pore of the CRAC channel. *Curr Biol* 2006;16:2073–2079. [PubMed: 16978865]
13. Yeromin AV, Zhang SL, Jiang W, Yu Y, Safrina O, Cahalan MD. Molecular identification of the CRAC channel by altered ion selectivity in a mutant of Orai. *Nature* 2006;443:226–229. [PubMed: 16921385]
14. Feske S, Prakriya M, Rao A, Lewis RS. A severe defect in CRAC  $Ca^{2+}$  channel activation and altered  $K^{+}$  channel gating in T cells from immunodeficient patients. *J Exp Med* 2005;202:651–662. [PubMed: 16147976]
15. Williams RT, Manji SS, Parker NJ, et al. Identification and characterization of the STIM (stromal interaction molecule) gene family: coding for a novel class of trans-membrane proteins. *Biochem J* 2001;357:673–685. [PubMed: 11463338]
16. Stathopoulos PB, Zheng L, Li GY, Plevin MJ, Ikura M. Structural and mechanistic insights into STIM1-mediated initiation of store-operated calcium entry. *Cell* 2008;135:110–122. [PubMed: 18854159]
17. de Villartay JP, Lim A, Al-Mousa H, et al. A novel immunodeficiency associated with hypomorphic RAG1 mutations and CMV infection. *J Clin Invest* 2005;115:3291–3299. [PubMed: 16276422]

18. Luik RM, Wang B, Prakriya M, Wu MM, Lewis RS. Oligomerization of STIM1 couples ER calcium depletion to CRAC channel activation. *Nature* 2008;454:538–542. [PubMed: 18596693]
19. Liou J, Fivaz M, Inoue T, Meyer T. Live-cell imaging reveals sequential oligomerization and local plasma membrane targeting of stromal interaction molecule 1 after Ca<sup>2+</sup> store depletion. *Proc Natl Acad Sci U S A* 2007;104:9301–9306. [PubMed: 17517596]
20. Baba Y, Nishida K, Fujii Y, Hirano T, Hikida M, Kurosaki T. Essential function for the calcium sensor STIM1 in mast cell activation and anaphylactic responses. *Nat Immunol* 2008;9:81–88. [PubMed: 18059272]
21. Oh-Hora M, Yamashita M, Hogan PG, et al. Dual functions for the endoplasmic reticulum calcium sensors STIM1 and STIM2 in T cell activation and tolerance. *Nat Immunol* 2008;9:432–443. [PubMed: 18327260]
22. Varga-Szabo D, Braun A, Kleinschnitz C, et al. The calcium sensor STIM1 is an essential mediator of arterial thrombosis and ischemic brain infarction. *J Exp Med* 2008;205:1583–1591. [PubMed: 18559454]
23. Stiber J, Hawkins A, Zhang ZS, et al. STIM1 signalling controls store-operated calcium entry required for development and contractile function in skeletal muscle. *Nat Cell Biol* 2008;10:688–697. [PubMed: 18488020]
24. Mühlemann O, Eberle AB, Stalder L, Zamudio Orozco R. Recognition and elimination of nonsense mRNA. *Biochim Biophys Acta* 2008;1779:538–549. [PubMed: 18657639]
25. Feske S, Giltzane J, Dolmetsch R, Staudt LM, Rao A. Gene regulation mediated by calcium signals in T lymphocytes. *Nat Immunol* 2001;2:316–324. [Erratum, *Nat Immunol* 2008;9:328-9.]. [PubMed: 11276202]
26. Partiseti M, Le Deist F, Hivroz C, Fischer A, Korn H, Choquet D. The calcium current activated by T cell receptor and store depletion in human lymphocytes is absent in a primary immunodeficiency. *J Biol Chem* 1994;269:32327–32335. [PubMed: 7798233]
27. Le Deist F, Hivroz C, Partiseti M, et al. A primary T-cell immunodeficiency associated with defective transmembrane calcium influx. *Blood* 1995;85:1053–1062. [PubMed: 7531512]
28. Wu Y, Borde M, Heissmeyer V, et al. FOXP3 controls regulatory T cell function through cooperation with NFAT. *Cell* 2006;126:375–387. [PubMed: 16873067]
29. Ochs HD, Gambineri E, Torgerson TR. IPEX, FOXP3 and regulatory T-cells: a model for autoimmunity. *Immunol Res* 2007;38:112–121. [PubMed: 17917016]
30. Gwack Y, Srikanth S, Oh-Hora M, et al. Hair loss and defective T-and B-cell function in mice lacking ORAI1. *Mol Cell Biol* 2008;28:5209–5222. [PubMed: 18591248]

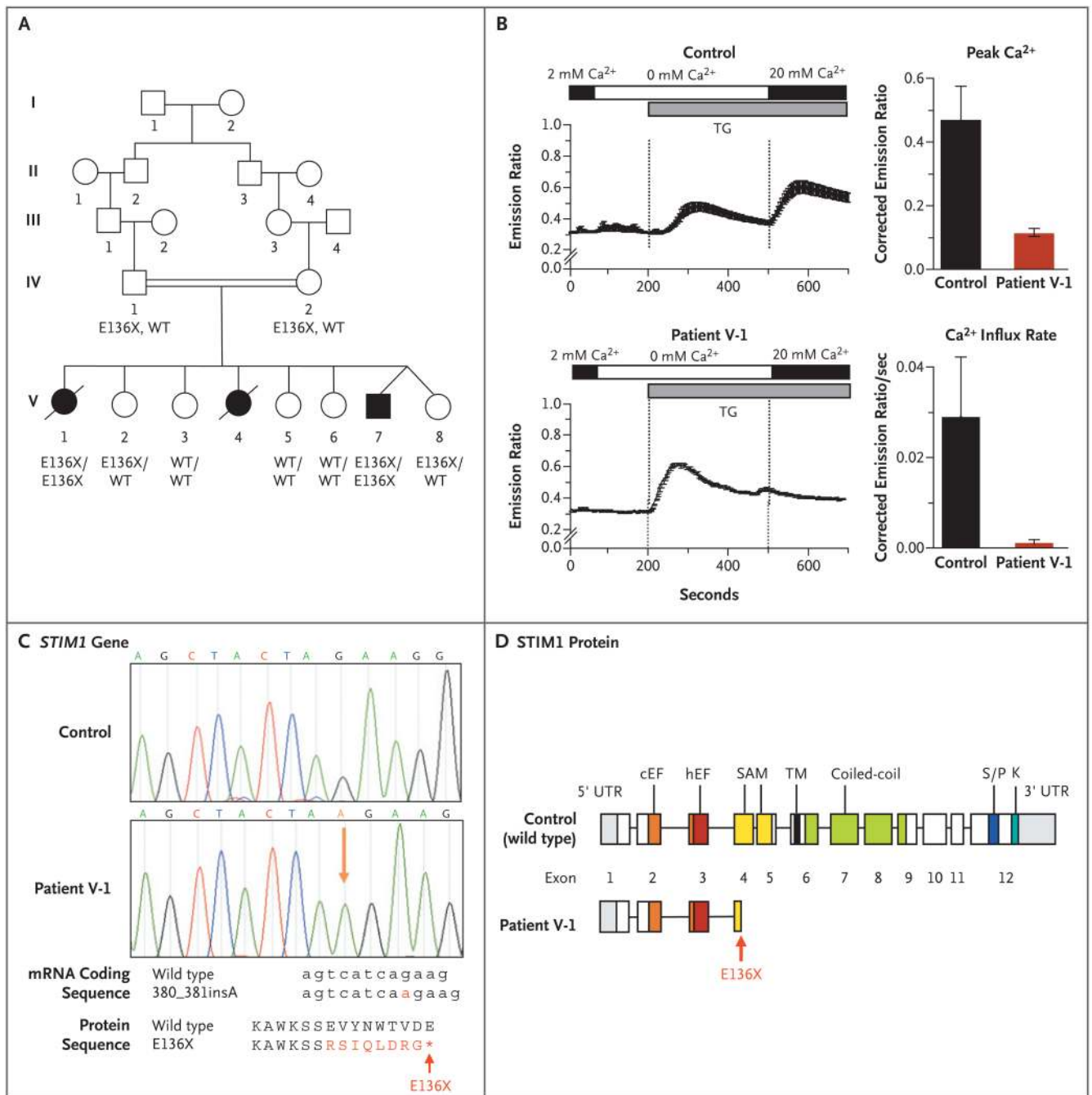


**Figure 1. Nonsense Mutation in the Stromal Interaction Molecule 1 Gene (*STIM1*) and Lack of Store-Operated Ca<sup>2+</sup> Entry into Cells**

Panel A shows the pedigree of the proband with combined immunodeficiency disease (Patient V-1) and her affected siblings (Patients V-4 and V-7). The *STIM1* genotypes of patients and family members from whom DNA was available for sequence analysis (all of whom were in generation IV or V) are listed under their symbols; no DNA was available for Patient V-4. WT denotes wild type. Squares indicate male family members, circles female family members, solid symbols patients, open symbols unaffected persons, slashes deceased persons, and double horizontal lines consanguinity. Panel B shows intracellular calcium levels measured in fibroblasts from Patient V-1 and from a control, showing a reduction of Ca<sup>2+</sup> influx in



fibroblasts from Patient V-1. Depletion of  $\text{Ca}^{2+}$  stores was induced with thapsigargin (TG) in  $\text{Ca}^{2+}$ -free Ringer's solution, followed by perfusion with Ringer's solution containing 20 mM  $\text{Ca}^{2+}$  to allow for  $\text{Ca}^{2+}$  influx. The resultant intracellular  $\text{Ca}^{2+}$  levels were measured as the ratio of fluorescence emissions at 510 nm of Fura-2, a fluorescent dye that binds calcium, after excitation at 340 nm and 380 nm, respectively. Between 40 and 80 cells per experiment were analyzed; results of one representative experiment are shown in the plots on the left side, in which the horizontal bars indicate the durations of perfusion with  $\text{Ca}^{2+}$ -containing (black) and  $\text{Ca}^{2+}$ -free (white) Ringer's solution and the duration of stimulation with thapsigargin (gray). The plots to the right show the average peak  $\text{Ca}^{2+}$  levels and initial  $\text{Ca}^{2+}$  influx rates after the perfusion of 20 mM  $\text{Ca}^{2+}$  (corrected for the baseline values, which were those before the initial depletion of the  $\text{Ca}^{2+}$  stores) from four independent experiments. I bars represent the standard error. Panel C shows the results of sequence analysis of genomic STIM1 DNA obtained from Patient V-1 and from a control, revealing an insertion of a single adenine in STIM1 exon 3, between positions 380 and 381 of the coding sequence (380\_381insA; NM\_003156) resulting in a frame shift and premature termination codon (X) at position 136 of the protein (E136X; NP\_003147). The structures of the STIM1 protein domains are superimposed on the sequence of STIM1 exons (modified from Williams et al.15) in Panel D, showing the location of the E136X truncation mutation in STIM1 exon 3, resulting in a truncated STIM1 protein in the N-terminal end of its sterile alpha-motif (SAM) domain. The abbreviation cEF denotes canonical EF-hand domain, hEF hidden EF-hand domain (as recently identified by Stathopoulos et al. 16), K lysine-rich domain, S/P serine-proline-rich domain, TM transmembrane domain, and UTR untranslated region.

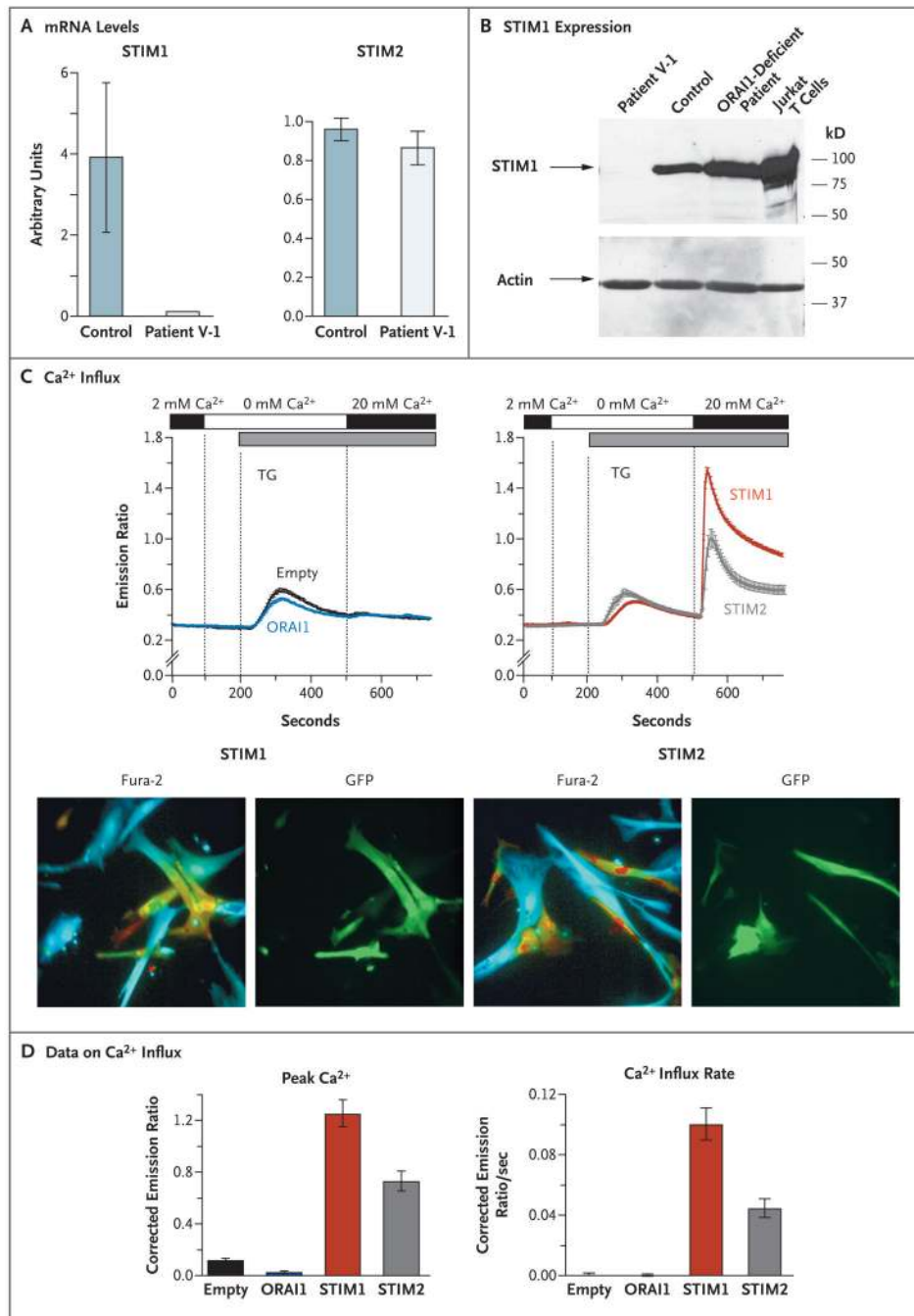


**Figure 2. Absence of Functional Stromal Interaction Molecule 1 (STIM1) in Fibroblasts and Restoration of Ca<sup>2+</sup> Influx with Addition of Exogenous STIM1 and STIM2**

Panel A shows the *STIM1* messenger RNA (mRNA) levels in fibroblasts from controls and Patient V-1. Quantitative real-time PCR was performed on complementary DNA (cDNA) from Patient V-1's fibroblasts and from control fibroblast cell lines (seven lines for the *STIM1* experiments and one line for the *STIM2* experiments), amplified with the use of primers specific for *STIM1*, *STIM2*, and the gene encoding glyceraldehyde-3-phosphate dehydrogenase (GAPDH). Threshold cycles ( $C_T$ ) for *STIM1* and *STIM2* expression, normalized to those of GAPDH ( $\Delta C_T$ ), are plotted as  $0.5^{\Delta C_T} \times 10^4$  (arbitrary units). The experiments were run in triplicate; results from one representative experiment are shown. The

I bars indicate the standard error. Panel B shows the STIM1 protein expression, as detected on Western blotting, in fibroblasts from Patient V-1, a control, and a previously described patient with ORAI1 deficiency (due to an R91W mutation),<sup>8</sup> as well as Jurkat T cells that were known to express STIM1 (derived from a patient with T-cell acute lymphoblastic leukemia). Total cell lysates were separated by means of sodium dodecyl sulfate–polyacrylamide gel electrophoresis and incubated with an affinity-purified antibody against the C-terminal domain of STIM1. Actin expression (as measured after incubating separated cell lysates with anti-actin antibody) is shown as a control, indicating equal loading. In Panel C (top), store-operated  $\text{Ca}^{2+}$  entry in fibroblasts from Patient V-1 is shown to be restored after transduction with bicistronic retroviral vectors expressing full-length STIM1 or STIM2 (right) but not after transduction with an empty vector (no insert) or a vector expressing ORAI1 (left). All vectors contained an internal ribosome entry site green fluorescent protein (GFP) cassette for the detection of transduced cells.  $\text{Ca}^{2+}$  measurements were obtained, and are presented, as described in Figure 1B. Between 20 and 40 cells per experiment were analyzed. Panel C (bottom) shows representative results for fibroblasts from Patient V-1 transduced with STIM1 or STIM2 vectors promoting bicistronic GFP expression. The Fura-2 images show pseudocolored intracellular  $\text{Ca}^{2+}$  levels: blue represents low  $\text{Ca}^{2+}$ , green intermediate  $\text{Ca}^{2+}$ , and yellow–red high  $\text{Ca}^{2+}$ . The GFP images show cells expressing GFP from an internal ribosome entry site, indicative of simultaneous STIM1 or STIM2 expression. In contrast to nontransduced cells (not visible in the GFP images), transduced cells (green) show high intracellular  $\text{Ca}^{2+}$  levels. Panel D shows the average (from between three and five experiments) peak  $\text{Ca}^{2+}$  level and initial rate of  $\text{Ca}^{2+}$  influx in fibroblasts from Patient V-1 containing empty vectors or vectors expressing ORAI1, STIM1, or STIM2. The data shown were measured after the addition of 20 mM of  $\text{Ca}^{2+}$  at 500 seconds. In Panel D, the I bars indicate the standard error.

Table 1

Characteristics of Patients with STIM1 Deficiency.\*

Characteristic	Patient V-1	Patient V-4	Patient V-7
Year of birth	1991	1994	2002
Sex	Female	Female	Male
STIM1 mutation <sup>†</sup>	E136X (both alleles)	Not known	E136X (both alleles)
Clinical manifestations			
Infection or related symptoms or therapy	Infection with <i>Escherichia coli</i> and <i>Streptococcus pneumoniae</i> , resulting in sepsis; urinary tract infections; pneumonia; infection with CMV and VZV	Infection with EBV, enteroviral encephalitis, prolonged diarrhea	Undocumented sepsis; treatment with IV immune globulin since birth
Autoimmune disorder	Hemolytic anemia, thrombocytopenia	Hemolytic anemia, thrombocytopenia	Thrombocytopenia
Lymphoproliferative disorder	Lymphadenopathy, hepatosplenomegaly	Lymphadenopathy, hepatosplenomegaly	None
Other	Muscular hypotonia, partial iris hypoplasia, abnormal dental enamel	Muscular hypotonia, partial iris hypoplasia, abnormal dental enamel, nephrotic syndrome	Muscular hypotonia, partial iris hypoplasia, abnormal dental enamel, hypoglycemia
Follow-up data	Died at 9 yr from HSCT complications	Died at 18 mo from encephalitis	HSCT performed at 15 mo; patient currently alive and well with muscular hypotonia
Immunologic features			
Lymphocyte count — $\times 10^{-3}/\mu\text{l}$ (normal range)	2.2 (2.3–5.7)	7.0 (3.9–9.0)	3.9 (3.9–9.0)
T cell population — % (normal range)			
CD3+	<b>83</b> (56–76)	55 (49–76)	63 (49–76)
CD4+	48 (28–47)	45 (31–56)	50 (31–56)
CD8+	29 (16–35)	<b>8</b> (12–24)	<b>9</b> (12–24)
CD4+CD45RA+	<b>24</b> (53–86)	NM	NM
CD4+CD45RA+CD31+	<b>14</b> (43–55)	NM	NM
CD4+FOXP3+	<b>0.3</b> (2.5–6.0)	NM	NM
Natural killer CD56+CD16+ cells — % (normal range)	NM	NM	12 (3–15)
B-cell CD19+ cells — % (normal range)	8 (6–35)	37 (14–37)	21 (14–37)
T-cell proliferation after stimulation — $\times 10^{-3}$ cpm (normal threshold) <sup>‡</sup>			
With PHA	<b>43</b> (>50)	NM	<b>7</b> (>50)
With PMA and ionomycin	<b>26</b> (>100)	NM	NM
With anti-CD3 antibody	<b>2</b> (>30)	NM	<b>0</b> (>30)
With anti-CD3 antibody and interleukin-2	<b>46</b> (>50)	NM	NM

Characteristic	Patient V-1	Patient V-4	Patient V-7
With VZV	<b>0</b> (>10)	NM	NM
With tetanus toxoid	NM	NM	<b>0.3</b> (>10)
Immunoglobulin — mg/dl (normal range) <sup>§</sup>			
IgG	<b>1700</b> (900–1480)	<b>46</b> (230–623)	336 (230–623)
IgA	<b>71</b> (110–260)	70 (20–86)	<b>109</b> (20–86)
IgM	<b>82</b> (88–180)	<b>23</b> (34–136)	44 (34–136)

\* All ranges and thresholds are adjusted for age. Values that are considerably outside the normal range are shown in bold. CMV denotes cytomegalovirus, cpm counts per minute, EBV Epstein–Barr virus, HSCT hematopoietic stem-cell transplantation, IV intravenous, NM not measured, PHA phytohemagglutinin, PMA phorbol 12-myristate 13-acetate, STIM1 stromal interaction molecule 1, and VZV varicella–zoster virus.

<sup>†</sup> DNA samples from Patient V-4 were not available for genotyping. The “X” in “E136X” denotes a premature stop codon.

<sup>‡</sup> T cells obtained from Patients V-1 and V-7 did not proliferate in response to stimulation with VZV and tetanus toxoid in vitro despite two episodes of chickenpox (in Patient V-1) and one round of vaccination against diphtheria, pertussis, and tetanus 1 month before the testing of the response to recall antigens (in Patient V-7).

<sup>§</sup> The immunoglobulin levels of Patient V-4 were measured after the onset of the nephrotic syndrome.